Journal of Computational and Applied Mathematics 235 (2011) 4350–4367

Contents lists available at ScienceDirect

Journal of Computational and Applied Mathematics

journal homepage: www.elsevier.com/locate/cam

The Trefftz method using fundamental solutions for biharmonic equations

Zi-Cai Li [a,b], Ming-Gong Lee [c], John Y. Chiang [b,*], Ya Ping Liu [d]

[a] Department of Applied Mathematics, National Sun Yat-sen University, Kaohsiung, 80424, Taiwan

[b] Department of Computer Science and Engineering, National Sun Yat-sen University, Kaohsiung, 80424, Taiwan

[c] Department of Applied Statistics, Chung-Hua University, HsinChu, Taiwan

[d] Mathematical College, Sichuan University, Chengdu, 610064, China

ARTICLE INFO

Article history:
Received 18 September 2009
Received in revised form 23 February 2011

Keywords:
Method of fundamental solutions
Almansi's fundamental solutions
Biharmonic equation
Singularity problem
Trefftz method
Error and stability analysis

ABSTRACT

In this paper, the Trefftz method of fundamental solution (FS), called the method of fundamental solution (MFS), is used for biharmonic equations. The bounds of errors are derived for the MFS with Almansi's fundamental solutions (denoted as the MAFS) in bounded simply connected domains. The exponential and polynomial convergence rates are obtained from highly and finitely smooth solutions, respectively. The stability analysis of the MAFS is also made for circular domains. Numerical experiments are carried out for both smooth and singularity problems. The numerical results coincide with the theoretical analysis made. When the particular solutions satisfying the biharmonic equation can be found, the method of particular solutions (MPS) is always superior to the MFS and the MAFS, based on numerical examples. However, if such singular particular solutions near the singular points do not exist, the local refinement of collocation nodes and the greedy adaptive techniques can be used for seeking better source points. Based on the computed results, the MFS using the greedy adaptive techniques may provide more accurate solutions for singularity problems. Moreover, the numerical solutions by the MAFS with Almansi's FS are slightly better in accuracy and stability than those by the traditional MFS. Hence, the MAFS with the AFS is recommended for biharmonic equations due to its simplicity.

1. Description of MFS

For simplicity, first consider the homogeneous biharmonic equation with the clamped boundary conditions

$$\Delta^2 u = 0 \quad \text{in } S, \tag{1.1}$$

$$u = f \quad \text{on } \Gamma, \tag{1.2}$$

$$u_\nu = g \quad \text{on } \Gamma, \tag{1.3}$$

where $\Delta = \frac{\partial^2}{\partial x^2} + \frac{\partial^2}{\partial y^2}$, S is the bounded simply connected domain, $u_\nu = \frac{\partial u}{\partial \nu}$ is the outward normal derivative to Γ, Γ is its boundary, and f and g are the known functions smooth enough. In real application, we may encounter the non-homogeneous equation $\Delta^2 u = p(x, y)$ in S. Suppose that a particular solution $\bar{u}$ is found so that $\Delta^2 \bar{u} = p(x, y)$ in S. By means of a transformation $w = u - \bar{u}$ we have the homogeneous biharmonic equation $\Delta^2 w = 0$ in S with the clamped

* Corresponding author.
E-mail address: chiang@cse.nsysu.edu.tw (J.Y. Chiang).

0377-0427/$ – see front matter © 2011 Elsevier B.V. All rights reserved.
doi:10.1016/j.cam.2011.03.024

boundary conditions $w = \bar{f} = f - \bar{u}$ on Γ and $w_\nu = \bar{g} = g - \bar{u}_\nu$ on Γ. Hence we may simply consider (1.1)–(1.3). The general solutions of biharmonic equations can be represented by

$$u = u(\rho, \theta) = \rho^2 v + z, \tag{1.4}$$

where (ρ, θ) are the polar coordinates, and v and z are the harmonic functions. Denote $r = |\overline{PQ}|$, $P = \rho e^{i\theta}$, $Q = Re^{i\varphi}$, φ is a radian with $0 \le \varphi \le 2\pi$, and $i = \sqrt{-1}$. Then $r = \sqrt{R^2 + \rho^2 - 2R\rho\cos(\theta - \varphi)}$. Hence the fundamental solutions of biharmonic equations in 2D are found from (1.4) as

$$\Phi(\rho, \theta) = r^2 \ln r = (R^2 + \rho^2 - 2R\rho\cos(\theta - \varphi)) \ln \sqrt{R^2 + \rho^2 - 2R\rho\cos(\theta - \varphi)}. \tag{1.5}$$

Denote

$$\Phi_j(\rho, \theta) = r_j^2 \ln r_j, \tag{1.6}$$

$$\phi_j(\rho, \theta) = \ln r_j, \tag{1.7}$$

where $r_j = |\overline{PQ_j}| = \sqrt{R^2 + \rho^2 - 2R\rho\cos(\theta - \varphi_j)}$ and $Q_j = Re^{i\varphi_j}$ with $\varphi_j \in [0, 2\pi]$. Hence we may choose the linear combinations of (1.6) and (1.7):

$$v_N = \sum_{j=1}^{N} \{c_j \Phi_j(\rho, \theta) + d_j \phi_j(\rho, \theta)\}, \tag{1.8}$$

where c_j and d_j are the unknown coefficients to be determined by the boundary conditions (1.2) and (1.3). We may use the Trefftz method [1]. Denote V_N the set of (1.8). Then the Trefftz solution u_N is obtained by

$$I(u_N) = \min_{v \in V_N} I(v), \tag{1.9}$$

where the energy

$$I(v) = \int_\Gamma (v - f)^2 + w^2 \int_\Gamma (v_\nu - g)^2, \tag{1.10}$$

ν is the normal of Γ, and w is the weight chosen as $w = 1/N$ in computation.

Almansi's fundamental solutions (simply denoted Almansi's FS) for biharmonic equations are obtained directly from (1.4).

Then Almansi's FS is given by

$$\Phi^A(\rho, \theta) = \rho^2 \ln \sqrt{R^2 + \rho^2 - 2R\rho\cos(\theta - \varphi)}, \tag{1.11}$$

while the fundamental solutions (1.5) are called the traditional FS in this paper. We may choose the linear combination of (1.11) and (1.7):

$$v_N^A = \sum_{j=1}^{N} \{c_j \Phi_j^A(\rho, \theta) + d_j \phi_j(\rho, \theta)\}, \tag{1.12}$$

to replace (1.8), where

$$\begin{aligned} \Phi_j^A(\rho, \theta) &= \rho^2 \ln r_j \\ &= \rho^2 \ln \sqrt{R^2 + \rho^2 - 2R\rho\cos(\theta - \varphi_j)}. \end{aligned} \tag{1.13}$$

The coefficients c_j and d_j can also be obtained from the Trefftz method (1.9). For the biharmonic equation, the MFS and numerical experiments are carried out for (1.8) and (1.12) in [2–5]. The other kind of fundamental solution is also introduced in [2].

Next, let us consider the mixed type of the clamped and simply support boundary conditions on Γ. Then Eq. (1.3) is replaced by (see [6])

$$u_\nu = g \quad \text{on } \Gamma_1, \qquad u_{\nu\nu} = g^* \quad \text{on } \Gamma_2, \tag{1.14}$$

where $\Gamma_1 \cup \Gamma_2 = \Gamma$, and $\Gamma_1 \cap \Gamma_2 = \emptyset$. The admissible functions (1.8) and (1.12) remain, but the energy $I(v)$ in (1.9) is replaced by

$$I^*(v) = \int_\Gamma (v - f)^2 + w^2 \int_{\Gamma_1} (v_\nu - g)^2 + (w_1^*)^2 \int_{\Gamma_2} (v_{\nu\nu} - g^*)^2, \tag{1.15}$$

where the weight $w_1^* = w^2 = 1/N^2$.

Below, we take the FS in (1.8) for example, and formulate the collocation equations from (1.14). For Almansi's FS in (1.12), the formulation of collocation equations is similar. We have

$$u_N = u_N(\rho,\theta) = \sum_{j=1}^{N} c_j(r_j^2 \ln r_j) + \sum_{j=1}^{N} d_j \ln r_j$$
$$= \sum_{j=1}^{N}\{c_j\Phi_j(\rho,\theta) + d_j\phi_j(\rho,\theta)\}, \tag{1.16}$$

where c_j and d_j are the coefficients, and $r_j = |PQ_j|$. By following [7], we choose the uniform collocation nodes on an enlarged circle of $\partial S : Q_k = (R, \varphi_k)$, $\varphi_k = \frac{2\pi}{N}k$. Then we obtain the collocation equations for the mixed type of boundary conditions:

$$u_N(\rho_k,\theta_k) = \sum_{j=1}^{N} c_j\Phi_j(\rho_k,\theta_k) + \sum_{j=1}^{N} d_j\phi_j(\rho_k,\theta_k) = f(\rho_k,\theta_k), \quad (\rho_k,\theta_k) \in \Gamma, \tag{1.17}$$

$$w\frac{\partial}{\partial \nu}u_N(\rho_k,\theta_k) = w\sum_{j=1}^{N} c_j\frac{\partial}{\partial \nu}\Phi_j(\rho_k,\theta_k) + w\sum_{j=1}^{N} d_j\frac{\partial}{\partial \nu}\phi_j(\rho_k,\theta_k) = wg(\rho_k,\theta_k), \quad (\rho_k,\theta_k) \in \Gamma_1, \tag{1.18}$$

$$w^2\frac{\partial^2}{\partial \nu^2}u_N(\rho_k,\theta_k) = w^2\sum_{j=1}^{N} c_j\frac{\partial^2}{\partial \nu^2}\Phi_j(\rho_k,\theta_k) + w^2\sum_{j=1}^{N} d_j\frac{\partial^2}{\partial \nu^2}\phi_j(\rho_k,\theta_k) = w^2g^*(\rho_k,\theta_k), \quad (\rho_k,\theta_k) \in \Gamma_2, \tag{1.19}$$

where ν is the normal of Γ_1 and Γ_2, and $w = 1/N$.

This paper is organized as follows. In Section 2, the error bounds are derived for the MAFS with Almansi's FS, and in Section 3, the stability analysis of the MAFS is also made for circular domains. In Sections 4 and 5, numerical experiments are carried out for the smooth and singular problems, respectively. In the last section, a few remarks are made.

2. Error analysis for the MAFS with Almansi's FS

In this section, from [7,8] we will develop the error analysis of the MAFS with Almansi's FS for biharmonic equations with the clamped boundary conditions (1.2) and (1.3).

Denote two harmonic polynomials of degree n,

$$P_n^h(\rho,\theta) = \frac{a_0}{2} + \sum_{i=1}^{n}\rho^i(a_i\cos i\theta + b_i\sin i\theta), \tag{2.1}$$

$$P_n^H(\rho,\theta) = \frac{a_0^*}{2} + \sum_{i=1}^{n}\rho^i(a_i^*\cos i\theta + b_i^*\sin i\theta), \tag{2.2}$$

with the coefficients a_i, b_i, a_i^* and b_i^*. The biharmonic solutions can be denoted by

$$u_n = P_n^A + R_n^A, \tag{2.3}$$

where the biharmonic polynomials of degree $n+2$ and the residuals are given by

$$P_n^A = P_n^A(\rho,\theta) = \rho^2P_n^H(\rho,\theta) + P_n^h(\rho,\theta), \tag{2.4}$$

$$R_n^A = R_n^A(\rho,\theta) = \rho^2R_n^H(\rho,\theta) + R_n^h(\rho,\theta), \tag{2.5}$$

respectively. The boundary norm is defined by

$$\|v\|_B = \left\{\|v\|_{0,\Gamma}^2 + w^2\left\|\frac{\partial v}{\partial \nu}\right\|_{0,\Gamma}^2\right\}^{1/2}, \tag{2.6}$$

and the Sobolev norms in $H^k(S)$ are defined by

$$\|v\|_k = \|v\|_{k,S} = \left(\sum_{\ell=0}^{k}|v|_{\ell,S}^2\right)^{1/2}. \tag{2.7}$$

Suppose that the solution has the regularity property,

$$u \in H^p(S), \quad p \geq 3. \tag{2.8}$$

There exist the bounds for the residuals,

$$\|R_n^H(\rho,\theta)\|_{k,S}, \qquad \|R_n^h(\rho,\theta)\|_{k,S} \leq C\frac{1}{n^{p-k}}\|u\|_{p,S}, \quad k = 0, 1. \tag{2.9}$$

There exist the bounds for the function v satisfying $\Delta v = 0$,

$$\|v\|_{k,\Gamma} \le C\|v\|_{k+\frac{1}{2},S}, \qquad \left\|\frac{\partial v}{\partial \nu}\right\|_{k,\Gamma} \le C\|v\|_{k+\frac{3}{2},S}, \tag{2.10}$$

where C is a constant independent of v. Hence from $w = \frac{1}{N}$ and $N \asymp n$[1] in computation, we have

$$\|R_n^A\|_B \le \|R_n^A\|_{0,\Gamma} + w\left\|\frac{\partial}{\partial \nu}R_n^A\right\|_{0,\Gamma} \le C\{\|R_n^A\|_{\frac{1}{2},S} + w\|R_n^A\|_{\frac{3}{2},S}\} \le C\frac{1}{n^{p-\frac{1}{2}}}\|u\|_{p,S}. \tag{2.11}$$

From (1.10) we have

$$\|u - u_N^A\|_B = \inf_{v\in V_N}\|u - v\|_B. \tag{2.12}$$

Let $v = \bar{u}_N^A$, where $\bar{u}_N^A := \Sigma_N(P_n^A;\rho,\theta)$ is a special linear combination of (1.12) using Almansi's FS, to approximate the biharmoic polynomial P_n^A of degree $n+2$. Hence we obtain

$$\begin{aligned}\|u - u_N^A\|_B &\le \|u - \bar{u}_N^A\|_B \le \|P_n^A - \bar{u}_N^A\|_B + \|u - P_n^A\|_B \\ &= \|P_n^A - \Sigma_N(P_n^A;\rho,\theta)\|_B + \|R_n^A\|_B.\end{aligned} \tag{2.13}$$

Since the bounds of $\|R_n^A\|_B$ are given in (2.11), the important work is to find the bounds of $\|P_n^A - \Sigma_N(P_n^A;\rho,\theta)\|_B$. Since

$$0 < \rho_0 \le \rho \le \mathrm{C} \quad \text{in } \Gamma, \tag{2.14}$$

the errors

$$\|P_n^A - \Sigma_N(P_n^A;\rho,\theta)\|_B, \tag{2.15}$$

have, essentiality, the same bounds

$$\|P_n^h - \Sigma_N(P_n^h;\rho,\theta)\|_{0,\Gamma}, \tag{2.16}$$

for Laplace's equations.

Let $h = \frac{2\pi}{N}$ and $R \ne 1$. Choose the following two special linear combinations [8],

$$\bar{v}_N^h = \Sigma_N(P_n^h;\rho,\theta) = \sum_{k=1}^{N}\bar{d}_k^h\phi_k(\rho,\theta), \tag{2.17}$$

$$\bar{v}_N^H = \Sigma_N(P_n^H;\rho,\theta) = \sum_{k=1}^{N}\bar{d}_k^H\phi_k(\rho,\theta), \tag{2.18}$$

where the coefficients are given explicitly by

$$\bar{d}_k^h = \frac{\alpha_{k,0}a_0}{2} + \sum_{m=1}^{n}(\alpha_{k,m}a_m + \beta_{k,m}b_m), \tag{2.19}$$

$$\bar{d}_k^H = \frac{\alpha_{k,0}a_0^*}{2} + \sum_{m=1}^{n}(\alpha_{k,m}a_m^* + \beta_{k,m}b_m^*), \tag{2.20}$$

and

$$\alpha_{k,0} = \frac{h}{2\pi\ln R}, \qquad \alpha_{k,m} = h\frac{mR^m}{\pi}\cos mk\pi, \quad m = 1,2,\ldots, \tag{2.21}$$

$$\beta_{k,m} = h\frac{mR^m}{\pi}\sin mk\pi, \quad m = 1,2,\ldots. \tag{2.22}$$

By following Li [7,8], we have the following lemma.

Lemma 2.1. *Let (2.14) hold and N satisfy*

$$2^{2q+1}\left(\frac{R}{r_{\min}}\right)^{-2N} \le 1. \tag{2.23}$$

[1] The notation $N \asymp n$ or $N \asymp O(n)$ denotes that there exist two constants C_1 and C_2 such that $C_1 n \le N \le C_2 n$.

For P_n^H and P_n^h there exist the bounds,

$$\|P_n^H - \Sigma_N(P_n^H;\rho,\theta)\|_{q,\Gamma} \le CN^q \left(\frac{R}{r_{\max}}\right)^{2n-N} \left(\frac{r_{\max}}{r_{\min}}\right)^n \|P_n^H\|_{0,\Gamma}, \tag{2.24}$$

$$\left\|\frac{\partial}{\partial\nu}\{P_n^H - \Sigma_N(P_n^H;\rho,\theta)\}\right\|_{q,\Gamma} \le CN^{q+1} \left(\frac{R}{r_{\max}}\right)^{2n-N} \left(\frac{r_{\max}}{r_{\min}}\right)^n \|P_n^H\|_{0,\Gamma}, \tag{2.25}$$

where $r_{\max} = \max r|_\Gamma$, $r_{\min} = \min r|_\Gamma$ and C is a constant independent of N and n.

Lemma 2.2. *Let (2.14) hold. There exist the bounds,*

$$\|\rho^2 P_n^H - \Sigma_N(\rho^2 P_n^H;\rho,\theta)\|_{k,\Gamma} \le C\|P_n^H - \Sigma_N(P_n^H;\rho,\theta)\|_{k,\Gamma}, \tag{2.26}$$

$$\left\|\frac{\partial}{\partial\nu}\{\rho^2 P_n^H - \Sigma_N(\rho^2 P_n^H;\rho,\theta)\}\right\|_{k,\Gamma} \le C\left\{\|P_n^H - \Sigma_N(P_n^H;\rho,\theta)\|_{k+1,\Gamma} + \left\|\frac{\partial}{\partial\nu}\{P_n^H - \Sigma_N(P_n^H;\rho,\theta)\}\right\|_{k,\Gamma}\right\}, \tag{2.27}$$

where C is a constant independent of N and n, and the linear combination of $\Phi_j(r,\theta)$ is given by

$$\Sigma_N(\rho^2 P_n^H;\rho,\theta) = \sum_{j=1}^{N} \bar{d}_j^H \Phi_j(\rho,\theta), \tag{2.28}$$

with the coefficients $\bar{d}_j^H$ in (2.20).

Proof. From (2.14) we have

$$\begin{aligned}\|\rho^2 P_n^H - \Sigma_N(\rho^2 P_n^H;\rho,\theta)\|_{k,\Gamma} &= \|\rho^2\{P_n^H - \Sigma_N(P_n^H;\rho,\theta)\}\|_{k,\Gamma}\\ &\le C\|P_n^H - \Sigma_N(P_n^H;r,\theta)\|_{k,\Gamma}.\end{aligned} \tag{2.29}$$

This is the first result (2.26). Next, there exist the derivative relations,

$$\frac{\partial v}{\partial\nu} = \frac{\partial v}{\partial\rho}\cos(\nu,\rho) + \frac{\partial v}{\rho\partial\theta}\cos(\nu,\theta) \tag{2.30}$$

$$\frac{\partial v}{\rho\partial\theta} = \frac{\partial v}{\partial\nu}\cos(\nu,\theta) + \frac{\partial v}{\partial s}\cos(s,\theta), \tag{2.31}$$

where ν and s are the normal and tangent directions of Γ, respectively. Let $v = \rho^2 P_n^H$, we have from (2.30) and (2.31)

$$\begin{aligned}\frac{\partial \rho^2 P_n^H}{\partial\nu} &= 2\rho P_n^H\cos(\nu,\rho) + \rho^2\left\{\frac{\partial}{\partial\rho}P_n^H\right\}\cos(\nu,\rho) + \rho^2\left\{\frac{\partial}{\rho\partial\theta}P_n^H\right\}\cos(\nu,\theta)\\ &= 2\rho P_n^H\cos(\nu,\rho) + \rho^2\left\{\frac{\partial}{\partial\rho}P_n^H\right\}\cos(\nu,\rho) + \rho^2\left\{\frac{\partial}{\partial\nu}P_n^H\right\}\cos^2(\nu,\theta) + \rho^2\left\{\frac{\partial}{\partial s}P_n^H\right\}\cos(s,\theta)\cos(\nu,\theta).\end{aligned} \tag{2.32}$$

Hence we obtain from (2.14)

$$\begin{aligned}\left\|\frac{\partial}{\partial\nu}\{\rho^2 P_n^H - \Sigma_N(\rho^2 P_n^H;\rho,\theta)\}\right\|_{k,\Gamma} &\le 2\max_\Gamma \rho\left\{\|\{P_n^H - \Sigma_N(P_n^H;\rho,\theta)\}\|_{k,\Gamma}\right.\\ &\quad\left. + \left\|\frac{\partial}{\partial\nu}\{P_n^H - \Sigma_N(P_n^H;\rho,\theta)\}\right\|_{k,\Gamma} + \|P_n^H - \Sigma_N(P_n^H;\rho,\theta)\|_{k+1,\Gamma}\right\}\\ &\le C\left\{\|P_n^H - \Sigma_N(P_n^H;\rho,\theta)\|_{k+1,\Gamma} + \left\|\frac{\partial}{\partial\nu}\{P_n^H - \Sigma_N(P_n^H;\rho,\theta)\}\right\|_{k,\Gamma}\right\}.\end{aligned} \tag{2.33}$$

This gives the second result (2.27), and completes the proof of Lemma 2.2. □

We have the following theorem.

Theorem 2.1. *Let (2.8), (2.14) and (2.23) hold. Then for $w = \frac{1}{N}$, there exists the bound,*

$$\|P_n^A - \Sigma_N(P_n^A;\rho,\theta)\|_B \le C\left(\frac{R}{r_{\max}}\right)^{2n-N}\left(\frac{r_{\max}}{r_{\min}}\right)^n, \tag{2.34}$$

where C is a constant independent of N and n, the special linear combination is given by

$$\bar{u}_N^A = \Sigma_N(P_n^A;\rho,\theta) = \sum_{j=1}^{N}(\bar{d}_j^H\Phi_j(\rho,\theta) + \bar{d}_j^h\phi_j(\rho,\theta)), \tag{2.35}$$

and $\bar{d}_j^H$ and $\bar{d}_j^h$ are given in (2.19) and (2.20), respectively.

Proof. First we have from (2.4),

$$\|P_n^A - \Sigma_N(P_n^A;\rho,\theta)\|_B \le \|\rho^2 P_n^H - \Sigma_N(\rho^2 P_n^H;\rho,\theta)\|_B + \|P_n^h - \Sigma_N(P_n^h;\rho,\theta)\|_B, \tag{2.36}$$

and from (2.6)

$$\|\rho^2 P_n^H - \Sigma_N(\rho^2 P_n^H;\rho,\theta)\|_B \le C\left\{\|\rho^2 P_n^H - \Sigma_N(\rho^2 P_n^H;\rho,\theta)\|_{0,\Gamma} + \frac{1}{N}\left\|\frac{\partial}{\partial\nu}\{\rho^2 P_n^H - \Sigma_N(\rho^2 P_n^H;\rho,\theta)\}\right\|_{0,\Gamma}\right\}. \tag{2.37}$$

From (2.8) and (2.3) we have $P_n^A \approx u$, and

$$\|P_n^A\|_B \le C\|u\|_B = O(1).$$

Hence from (2.4) and (2.14), there exist the bounds

$$\|P_n^H\|_{0,\Gamma}, \qquad \|P_n^h\|_{0,\Gamma} = O(1). \tag{2.38}$$

From (2.36)–(2.38) and Lemmas 2.1 and 2.2, we have

$$\begin{aligned}\|\rho^2 P_n^H(\rho,\theta) - \Sigma_N(\rho^2 P_n^H;\rho,\theta)\|_B &\le C\left(\frac{R}{r_{\max}}\right)^{2n-N}\left(\frac{r_{\max}}{r_{\min}}\right)^n \|P_n^H(\rho,\theta)\|_{0,\Gamma_0}\\ &\le C\left(\frac{R}{r_{\max}}\right)^{2n-N}\left(\frac{r_{\max}}{r_{\min}}\right)^n,\end{aligned} \tag{2.39}$$

and then from (2.36) and (2.38)

$$\begin{aligned}\|P_n^A - \Sigma_N(P_n^A;\rho,\theta)\|_B &\le \|\rho^2 P_n^H - \Sigma_N(\rho^2 P_n^H;\rho,\theta)\|_B + \|P_n^h - \Sigma_N(P_n^h;\rho,\theta)\|_B\\ &\le C\left(\frac{R}{r_{\max}}\right)^{2n-N}\left(\frac{r_{\max}}{r_{\min}}\right)^N \{\|P_n^H(\rho,\theta)\|_B + \|P_n^h(\rho,\theta)\|_B\}\\ &\le C\left(\frac{R}{r_{\max}}\right)^{2n-N}\left(\frac{r_{\max}}{r_{\min}}\right)^N.\end{aligned} \tag{2.40}$$

This completes the proof of Theorem 2.1. □

Theorem 2.2. *Let (2.8), (2.14) and (2.23) hold, and choose N such that*

$$\left(\frac{R}{r_{\max}}\right)^{2n-N}\left(\frac{r_{\max}}{r_{\min}}\right)^n = \frac{1}{n^{p-\frac{1}{2}}}. \tag{2.41}$$

Then when $w = \frac{1}{N}$, there exists the bound,

$$\|u - u_N^A\|_B \le C\frac{1}{N^{p-\frac{1}{2}}}, \tag{2.42}$$

where C is a constant independent of N and n.

Proof. From (2.13), (2.11) and Theorem 2.1, when $w = \frac{1}{N}$ we obtain the following error bound,

$$\|u - u_N^A\|_B \le C\left(\frac{R}{r_{\max}}\right)^{2n-N}\left(\frac{r_{\max}}{r_{\min}}\right)^n. \tag{2.43}$$

Under (2.41), Eq. (2.43) leads to

$$\|u - u_N^A\|_B \le C\frac{1}{n^{p-\frac{1}{2}}}. \tag{2.44}$$

For (2.41), we may choose

$$N \approx 2n + \frac{1}{\ln\left(\frac{R}{r_{\min}}\right)}\left\{n\frac{r_{\max}}{r_{\min}} + \left(p - \frac{1}{2}\right)\ln n\right\} \le Cn, \tag{2.45}$$

which implies $n \asymp N$. We have from (2.44)

$$\|u - u_N^A\|_B \le C\frac{1}{N^{p-\frac{1}{2}}}. \tag{2.46}$$

This completes the proof of Theorem 2.2. □

Note that Eq. (2.46) is similar to the bounds for Laplace's equation in [8]. Moreover, the H^1 errors in S may also be derived, to give the optimal convergence rate:

$$\|u - u_N\|_{1,S} = O\left(\frac{1}{N^{p-1}}\right), \tag{2.47}$$

provided that $u \in H^p(S)$ $(p \ge 3)$. When the solution is highly smooth, the exponential convergence rates can also be obtained. For the biharmonic equations with the mixed type of boundary conditions (1.14), the error bounds of the MAFS can also be derived, to give the polynomial convergence rates as in (2.46) and (2.47).

Remark 2.1. The error estimates of the MFS for (1.8) are more challenging and difficult, details appear in a subsequent paper, although the same error bounds as (2.46) and (2.47) are obtained.

3. Stability analysis on circular domains for the MAFS with Almansi's FS

We consider only the circular domains in this paper. For the non-circular domains, the stability analysis may follow [9]. From (1.8), we have

$$\begin{aligned} u_N &= u_N(\rho,\theta) = \sum_{j=1}^{N} c_j(\rho^2 \ln r_j) + \sum_{j=1}^{N} d_j \ln r_j \\ &= \sum_{j=1}^{N} c_j \Phi_j^A(\rho,\theta) + d_j\phi_j(\rho,\theta), \end{aligned} \tag{3.1}$$

where c_j and d_j are the coefficients, $r_j = |\overline{PQ_j}|$, $P = \rho e^{i\theta}$, $Q_j = Re^{i\varphi_j}$, $\varphi_j = \frac{2\pi}{N}j$, and $i = \sqrt{-1}$. We also choose the uniform collocation nodes at $P_k = \rho e^{i\theta_k}$ and $\theta_k = \frac{2\pi}{N}k$. Then we have the $2N$ collocation equations:

$$u_N(\rho,\theta_k) = \sum_{j=1}^{N} c_j \Phi_j^A(\rho,\theta_k) + \sum_{j=1}^{N} d_j\phi_j(\rho,\theta_k) = f(\rho,\theta_k), \tag{3.2}$$

$$w\frac{\partial}{\partial\rho}u_N(\rho,\theta_k) = w\sum_{j=1}^{N} c_j\frac{\partial}{\partial\rho}\Phi_j^A(\rho,\theta_k) + w\sum_{j=1}^{N} d_j\frac{\partial}{\partial\rho}\phi_j(\rho,\theta_k) = wg(\rho,\theta_k), \tag{3.3}$$

where $k = 1, 2, \ldots, N$, and w is a weight constant with $w = 1/N$. Hence the $2N$ coefficients c_j and d_j can be obtained by (3.2) and (3.3) if the system of equations is nonsingular, which will be confirmed in Lemma 3.3 given below. Denote (3.2) and (3.3) as the form of matrix and vector:

$$\mathbf{Ax} = \mathbf{b}, \tag{3.4}$$

where the vectors

$$\mathbf{x} = \{c_1, \ldots, c_N, d_1, \ldots, d_N\}^T, \tag{3.5}$$

$$\mathbf{b} = \{f_1, \ldots, f_N, wg_1, \ldots, wg_N\}^T, \tag{3.6}$$

and the matrix $\mathbf{A} \in R^{2N\times 2N}$ is decomposed as

$$\mathbf{A} = \begin{bmatrix} \mathbf{A}_{11}(\Phi) & \mathbf{A}_{12}(\phi) \\ w\mathbf{A}_{21}(D\Phi) & w\mathbf{A}_{22}(D\phi) \end{bmatrix}, \tag{3.7}$$

where

$$\mathbf{A}_{11}(\Phi) \in R^{N\times N} = \begin{bmatrix} \Phi_1^A(\theta_1) & \cdots & \Phi_N^A(\theta_1) \\ \vdots & \ddots & \vdots \\ \Phi_1^A(\theta_N) & \cdots & \Phi_N^A(\theta_N) \end{bmatrix},$$

$$\mathbf{A}_{12}(\phi) \in R^{N\times N} = \begin{bmatrix} \phi_1^A(\theta_1) & \cdots & \phi_N^A(\theta_1) \\ \vdots & \ddots & \vdots \\ \phi_1^A(\theta_N) & \cdots & \phi_N^A(\theta_N) \end{bmatrix},$$

$$\mathbf{A}_{21}(D\Phi) \in R^{N\times N} = \begin{bmatrix} \dfrac{\partial}{\partial\rho}\Phi_1^A(\theta_1) & \cdots & \dfrac{\partial}{\partial\rho}\Phi_N^A(\theta_1) \\ \vdots & \ddots & \vdots \\ \dfrac{\partial}{\partial\rho}\Phi_1^A(\theta_N) & \cdots & \dfrac{\partial}{\partial\rho}\Phi_N^A(\theta_N) \end{bmatrix},$$

$$\mathbf{A}_{22}(D\phi) \in R^{N\times N} = \begin{bmatrix} \dfrac{\partial}{\partial\rho}\phi_1^A(\theta_1) & \cdots & \dfrac{\partial}{\partial\rho}\phi_N^A(\theta_1) \\ \vdots & \ddots & \vdots \\ \dfrac{\partial}{\partial\rho}\phi_1^A(\theta_N) & \cdots & \dfrac{\partial}{\partial\rho}\phi_N^A(\theta_N) \end{bmatrix}. \tag{3.8}$$

The matrices $\mathbf{A}_{12}(\phi)$ and $\mathbf{A}_{22}(D\phi)$ result from the Dirichlet and Neumann problems of Laplace's equations on circular domains, given in [9], respectively. All four sub-matrices $A_{11}(\Phi), A_{12}(\phi), A_{21}(D\Phi)$ and $A_{22}(D\phi)$ are circulant. Denote the eigen-matrix (see [10], p.32)

$$\mathbf{F}^*(\in C^{N\times N}) = \frac{1}{\sqrt{N}}\begin{bmatrix} 1 & 1 & 1 & \cdots & 1 \\ 1 & \omega & \omega^2 & \cdots & \omega^{N-1} \\ 1 & \omega^2 & \omega^4 & \cdots & \omega^{2(N-1)} \\ \vdots & \vdots & \ddots & \vdots & \\ 1 & \omega^{N-1} & \omega^{2(N-1)} & \cdots & \omega^{(N-1)(N-1)} \end{bmatrix}, \tag{3.9}$$

where $\omega = \mathrm{e}^{\frac{2\pi}{N}\mathrm{i}} = \cos\frac{2\pi}{N} + \mathrm{i}\sin\frac{2\pi}{N}$, $\mathbf{F}$ is unitary with $\mathbf{F}\mathbf{F}^* = \mathbf{F}^*\mathbf{F} = \mathbf{I}$, and $\mathbf{I}$ is the identity matrix. Based on Davis [10], p. 73, we have

$$\mathbf{A}_{11}(\Phi) = \mathbf{F}^*\Lambda_{11}(\Phi)\mathbf{F}, \qquad \mathbf{A}_{12}(\phi) = \mathbf{F}^*\Lambda_{12}(\phi)\mathbf{F}, \tag{3.10}$$
$$\mathbf{A}_{21}(D\Phi) = \mathbf{F}^*\Lambda_{21}(D\Phi)\mathbf{F}, \qquad \mathbf{A}_{22}(D\phi) = \mathbf{F}^*\Lambda_{22}(D\phi)\mathbf{F}.$$

In (3.10), the matrices, $\Lambda_{11}(\Phi)$, $\Lambda_{12}(\phi)$, $\Lambda_{21}(D\Phi)$ and $\Lambda_{22}(D\phi)$, are diagonal. We have from [9]

$$\Lambda_{12}(\phi) = \begin{bmatrix} \lambda_0(\phi) & & 0 \\ & \ddots & \\ 0 & & \lambda_{N-1}(\phi) \end{bmatrix}, \tag{3.11}$$

$$\Lambda_{22}(D\phi) = \begin{bmatrix} \lambda_0(D\phi) & & 0 \\ & \ddots & \\ 0 & & \lambda_{N-1}(D\phi) \end{bmatrix}, \tag{3.12}$$

$$\Lambda_{11}(\Phi) = \begin{bmatrix} \lambda_0(\Phi) & & 0 \\ & \ddots & \\ 0 & & \lambda_{N-1}(\Phi) \end{bmatrix},$$

$$\Lambda_{21}(D\Phi) = \begin{bmatrix} \lambda_0(D\Phi) & & 0 \\ & \ddots & \\ 0 & & \lambda_{N-1}(D\Phi) \end{bmatrix}. \tag{3.13}$$

Since the eigenvalues of similar matrices are the same, the eigenvalues of $\mathbf{A}$ are just those of Λ, denoted by

$$\Lambda = \begin{bmatrix} \Lambda_{11}(\Phi) & \Lambda_{12}(\phi) \\ w\Lambda_{21}(D\Phi) & w\Lambda_{22}(D\phi) \end{bmatrix} = \begin{bmatrix} \mathrm{diag}(\lambda_i(\Phi)) & \mathrm{diag}(\lambda_i(\phi)) \\ w\mathrm{diag}(\lambda_i(D\Phi)) & w\mathrm{diag}(\lambda_i(D\phi)) \end{bmatrix}. \tag{3.14}$$

By using matrix $\mathbf{F}^*$ in (3.9), we obtain from (3.10)

$$\begin{aligned}\mathbf{A} &= \begin{bmatrix} \mathbf{A}_{11}(\Phi) & \mathbf{A}_{12}(\phi) \\ w\mathbf{A}_{21}(D\Phi) & w\mathbf{A}_{22}(D\phi) \end{bmatrix} \\ &= \begin{bmatrix} \mathbf{F}^* & O \\ O & \mathbf{F}^* \end{bmatrix} \begin{bmatrix} \Lambda_{11}(\Phi) & \Lambda_{12}(\phi) \\ w\Lambda_{21}(D\Phi) & w\Lambda_{22}(D\phi) \end{bmatrix} \begin{bmatrix} \mathbf{F} & O \\ O & \mathbf{F} \end{bmatrix}. \end{aligned} \tag{3.15}$$

By a permutation transformation $\mathbf{P}$,

$$\mathbf{P}^T \Lambda \mathbf{P} = \begin{bmatrix} \lambda_0(\Phi) & \lambda_0(\phi) & & & & & & \\ w\lambda_0(D(\phi)) & w\lambda_0(D\phi) & & & & & & \\ & & \ddots & & & & & \\ & & & \lambda_i(\Phi) & \lambda_i(\phi) & & & \\ & & & w\lambda_i(D\Phi) & w\lambda_i(D\phi) & & & \\ & & & & \ddots & & & \\ & & & & & \lambda_N(\Phi) & \lambda_N(\phi) \\ & & & & & w\lambda_N(D\Phi) & w\lambda_N(D\phi) \end{bmatrix}.$$

We have a lemma.

Lemma 3.1. *Let the eigenvalues of matrix ϕ be*

$$\lambda_k(\phi) = c_0 + c_1\rho^k + c_2\rho^{N-k}, \tag{3.16}$$

where c_0, c_1 and c_2 are constants independent of ρ. Then there exist the eigenvalues for matrices $\mathbf{D}\phi$, $\mathbf{\Phi}$ and $\mathbf{D\Phi}$,

$$\lambda_k(\mathbf{D}\phi) = c_1 k\rho^{k-1} + c_2(N-k)\rho^{N-k-1}, \tag{3.17}$$

$$\lambda_k(\mathbf{\Phi}) = c_0\rho^2 + c_1\rho^{k+2} + c_2\rho^{N-k+2}, \tag{3.18}$$

$$\lambda_k(\mathbf{D\Phi}) = 2c_0\rho + c_1(k+2)\rho^{k+1} + c_2(N-k+2)\rho^{N-k+1}. \tag{3.19}$$

Proof. Consider the matrix eigenvalue problem,

$$\mathbf{Bx} = \lambda\mathbf{x} \tag{3.20}$$

where $\mathbf{B}$ is the circulant matrix dependent of ρ, and the eigenvectors are given in (3.9). Since $\frac{\partial}{\partial\rho}(\mathbf{B})$, $\rho^2\mathbf{B}$ and $\frac{\partial}{\partial\rho}(\rho^2\mathbf{B})$ are also circulant, with the same eigenvectors, the conclusions (3.17)–(3.19) hold. □

Lemma 3.2. *For the matrix $\mathbf{A} \in R^{n\times n}$ with $n = 2N$ from MAFS, when $w = \frac{1}{N}$, $R \neq 1$ and $\rho < R$, there exist the leading eigenvalues*

$$\lambda_0^+ \asymp N, \quad \lambda_0^- \asymp 1, \tag{3.21}$$

Proof. Since the leading eigenvalue is given from [9] by

$$\lambda_0(\phi) = N\ln R + \varepsilon \approx N\ln R, \quad \varepsilon \approx -\left(\frac{\rho}{R}\right)^N,$$

we have

$$\lambda_0(D\phi) \approx 0, \qquad \lambda_0(\Phi) = \lambda_0(\rho^2\phi) \approx N\rho^2\ln R, \qquad \lambda_0(D\Phi) \approx 2N\rho\ln R.$$

Hence we obtain the matrix of the leading eigenvalue $\lambda_0^{\pm}$,

$$\begin{aligned}\begin{bmatrix} \lambda_0(\Phi) & \lambda_0(\phi) \\ w\lambda_0(D\Phi) & w\lambda_0(D\phi) \end{bmatrix} &\approx \begin{bmatrix} N\rho^2\ln R & N\ln R \\ w2\rho N\ln R & 0 \end{bmatrix} \\ &= \begin{bmatrix} N\rho^2\ln R & N\ln R \\ 2\rho\ln R & 0 \end{bmatrix} = \ln R \begin{bmatrix} N\rho^2 & N \\ 2\rho & 0 \end{bmatrix}. \end{aligned} \tag{3.22}$$

From (3.22) the leading eigenvalues are given by $\lambda_0^{\pm} = \mu^{\pm}\ln R$, where $\mu^{\pm}$ satisfy

$$\lambda^2 - N\rho^2\lambda - 2\rho N = 0,$$

to give

$$\lambda_0^{\pm} = \frac{\ln R}{2}\{N\rho^2 \pm \sqrt{N^2\rho^4 + 8\rho N}\}.$$

When $R \neq 1$ and N is large, we have

$$\lambda_0^+ \asymp N\rho^2, \qquad \lambda_0^- \asymp \frac{2}{\rho},$$

and the desired result (3.21) follow. □

Lemma 3.3. *Let all the conditions in Lemma 3.2 hold. Then there exists the minimal eigenvalue*

$$\min_k |\lambda_k(\mathbf{A})| \asymp \frac{1}{N}\left(\frac{\rho}{R}\right)^{\frac{N}{2}}. \tag{3.23}$$

Proof. The original eigenvalues are given in [9]

$$\lambda_k(\phi) \approx -\frac{N}{2}\left[\frac{1}{k}\left(\frac{\rho}{R}\right)^k + \frac{1}{N-k}\left(\frac{\rho}{R}\right)^{N-k}\right], \quad k = 1, 2, \ldots, N-1. \tag{3.24}$$

Based on Lemma 3.1 we have

$$\lambda_k(D\phi) \approx -\frac{N}{2\rho}\left[\left(\frac{\rho}{R}\right)^k + \left(\frac{\rho}{R}\right)^{N-k}\right], \tag{3.25}$$

$$\lambda_k(\Phi) = \rho^2\lambda_k(\phi) \approx -\frac{N\rho^2}{2}\left[\frac{1}{k}\left(\frac{\rho}{R}\right)^k + \frac{1}{N-k}\left(\frac{\rho}{R}\right)^{N-k}\right], \tag{3.26}$$

$$\lambda_k(D\Phi) = \frac{\partial}{\partial\rho}\lambda_k(\Phi) \approx -\frac{N\rho}{2}\left[\frac{k+2}{k}\left(\frac{\rho}{R}\right)^k + \frac{N-k+2}{N-k}\left(\frac{\rho}{R}\right)^{N-k}\right]. \tag{3.27}$$

Without loss of generality, let N be even. Let $k = \frac{N}{2}$ we obtain

$$\lambda_{\frac{N}{2}}(\phi) \approx -2\left(\frac{\rho}{R}\right)^{\frac{N}{2}}, \qquad \lambda_{\frac{N}{2}}(D\phi) \approx -\frac{N}{\rho}\left(\frac{\rho}{R}\right)^{\frac{N}{2}}, \tag{3.28}$$

$$\lambda_{\frac{N}{2}}(\Phi) \approx -2\rho^2\left(\frac{\rho}{R}\right)^{\frac{N}{2}}, \qquad \lambda_{\frac{N}{2}}(D\Phi) \approx -(N+4)\rho\left(\frac{\rho}{R}\right)^{\frac{N}{2}}. \tag{3.29}$$

Then we obtain the matrix at $k = \frac{N}{2}$ and $w = \frac{1}{N}$,

$$\begin{bmatrix} \lambda_k(\Phi) & \lambda_k(\phi) \\ w\lambda_k(D\Phi) & w\lambda_k(D\phi) \end{bmatrix} \approx \begin{bmatrix} -2\rho^2\left(\frac{\rho}{R}\right)^{\frac{N}{2}} & -2\left(\frac{\rho}{R}\right)^{\frac{N}{2}} \\ -w(N+4)\rho\left(\frac{\rho}{R}\right)^{\frac{N}{2}} & -w\frac{N}{\rho}\left(\frac{\rho}{R}\right)^{\frac{N}{2}} \end{bmatrix}$$
$$= -\left(\frac{\rho}{R}\right)^{\frac{N}{2}} \begin{bmatrix} 2\rho^2 & 2 \\ \left(1+\frac{4}{N}\right)\rho & \frac{1}{\rho} \end{bmatrix}. \tag{3.30}$$

The eigenvalues of (3.30) are given by $\lambda_{\frac{N}{2}}^{\pm} = -\left(\frac{\rho}{R}\right)^{\frac{N}{2}}\mu^{\pm}$, where $\mu^{\pm}$ satisfy the quadratic equation,

$$\lambda^2 - \left(2\rho^2 + \frac{1}{\rho}\right)\lambda - \frac{8\rho}{N} = 0. \tag{3.31}$$

Similarly we have

$$\mu^+ \asymp 1, \qquad \mu^- \asymp \frac{1}{N}. \tag{3.32}$$

Then the minimal eigenvalue is obtained by

$$\min_k |\lambda_k(\mathbf{A})| = |\lambda_{\frac{N}{2}}^-(\mathbf{A})| \asymp \frac{1}{N}\left(\frac{\rho}{R}\right)^{\frac{N}{2}}. \tag{3.33}$$

This is the desired result (3.23).

From Lemmas 3.2 and 3.3 we have the following theorem. □

Theorem 3.1. *Let all the conditions in Lemma 3.2 hold. Then there exists the bound*

$$\text{Cond} = \frac{\max\limits_k |\lambda_k(\mathbf{A})|}{\min\limits_k |\lambda_k(\mathbf{A})|} \le CN^2 \left(\frac{R}{\rho}\right)^{\frac{N}{2}}. \tag{3.34}$$

Theorem 3.1 is for the circular domains. For the bounded simply connected domains, the exponential bounds of condition number can also be derived by following the arguments in [9].

4. Plate bending problem with smooth solutions

Consider (1.1)–(1.3) in the rectangular domain $S = \{(x, y) | -1 < x < 1, \ -1 < y < 1\}$, and choose the true solution,

$$u(x, y) = \exp(x)\cos y + (x^2 + y^2)\exp(y)\cos x. \tag{4.1}$$

The plate bending problem with the mixed type of the clamped and simply supported boundary conditions is given in (1.14). For the collocation Eqs. (1.17)–(1.19), the number m of collocation nodes is often chosen to be larger than the number n of source nodes. Then we obtain the over-determined system of linear algebraic equations

$$\mathbf{A}\mathbf{x} = \mathbf{b}, \tag{4.2}$$

where the matrix $\mathbf{A} \in R^{m\times n}(m \ge n)$, $\mathbf{x} \in R^n$ and $\mathbf{b} \in R^m$. The traditional condition number is defined by

$$\text{Cond} = \frac{\sigma_{\max}}{\sigma_{\min}}, \tag{4.3}$$

where $\sigma_{\max}$ and $\sigma_{\min}$ are the maximal and the minimal singular value of the matrix $\mathbf{A}$, respectively. The new effective condition number is defined in [11,12] as

$$\text{Cond\_eff} = \frac{\|\mathbf{b}\|}{\sigma_{\min}\|\mathbf{x}\|}, \tag{4.4}$$

where $\|\mathbf{x}\|$ is the Euclidean norm. The boundary errors are given by

$$\|\epsilon\|_B = \|u - u_N\|_B = \sqrt{I(u_N)},$$

where

$$I(v) = \int_\Gamma (v - f)^2 + w_1^2 \int_{\Gamma_1} (v_\nu - g)^2 + w_2^2 \int_{\Gamma_2} (v_{\nu\nu} - g^*)^2,$$

with $w_i = 1/N^i$. When $\Gamma_2 = \emptyset$, the mixed type is just the purely clamped boundary conditions. We use both the traditional MFS with (1.8) and the MAFS with Almansi's FS with (1.12). For the clamped boundary conditions, the errors and condition numbers are listed in Tables 1 and 2, where M denotes the number of uniform collocation nodes along each edge of ∂S. Then $n = 2N$ and $m = 8M$ in (4.2). We also use the Trefftz method with the particular solutions (2.4), to give the method of particular solutions (MPS), and their results are listed in Table 3. Interestingly, the numerical solutions of the MAFS are slightly better than those of the MFS. However, the MPS is superior to both the MFS and the MAFS.

Next, we still choose the true solution (4.1), but use the mixed type of the clamped and simply supported boundary conditions:

$$\begin{aligned} &u = f, \qquad u_\nu = g, \quad \text{on } x = \pm 1, \\ &u = f, \qquad u_{\nu\nu} = g^*, \quad \text{on } y = \pm 1, \end{aligned} \tag{4.5}$$

where ν is the exterior normal of ∂S. The errors and condition numbers of the MFS, the MAFS and the MPS are listed in Tables 4–6. All tables and figures are carried out by Java programs with double precision. The errors of the MFS and the MAFS are larger than those of the MPS, because their huge Cond and Cond_eff adversely affect the accuracy of numerical solutions.

From the above tables and figures, we may also conclude that for smooth solutions, the errors of the MFS may catch up with those of MPS, if the huge effective condition numbers will not deteriorate the accuracy in the sense that there exist the sufficient significant digits for the numerical solutions obtained. Evidently, it is due to better stability that the MPS is superior to the MFS and the MAFS.

5. Plate bending problem with crack singularity

5.1. The MFS using uniform source points on the enlarged circle

Consider the homogeneous biharmonic equation $\Delta^2 u = 0$ in S, where the solution domain is also a rectangle: $S : \{(x, y) \mid -1 < x < 1, 0 < y < 1\}$. We choose a crack model of singularity from [6], shown in Fig. 1. The section $\overline{OD}$ represents an interior crack under the clamped conditions: $u = u_\nu = 0$. The symmetric conditions, $u_\nu = u_{\nu\nu\nu} = 0$ on $\overline{OA} \cup \overline{BC} \cup \overline{CD}$, are

Table 1
Errors and condition numbers for the biharmonic equation with the clamped boundary condition by the MFS and the MAFS with $R = 2.0$, where $\epsilon = u - u_N$ or $\epsilon = u - u_N^A$.

	N	M	$\|\epsilon\|_B$	$\|\epsilon\|_{0,S}$	$\|\epsilon\|_{1,S}$	Cond	Cond_eff	$\|\mathbf{x}\|$
MFS	11	5	2.25(−1)	8.77(−2)	6.08(−1)	1.54(4)	86.0	27.3
	21	10	2.16(−3)	4.46(−4)	6.89(−3)	1.28(6)	5.95(3)	23.6
	31	15	2.89(−5)	4.33(−6)	9.07(−5)	4.10(7)	1.89(5)	19.6
	41	20	6.03(−7)	3.72(−8)	1.94(−6)	1.32(9)	6.24(6)	16.6
MAFS with Almansi's FS	11	5	6.44(−2)	1.78(−2)	1.46(−1)	1.13(3)	1.62(2)	4.64
	21	10	4.40(−4)	9.18(−5)	1.53(−3)	4.05(4)	6.49(3)	2.99
	31	15	5.62(−6)	8.06(−7)	1.47(−5)	7.85(5)	1.26(5)	2.44
	41	20	1.37(−7)	8.25(−9)	4.14(−7)	1.79(7)	2.89(6)	2.12

Table 2
Errors and condition numbers for the biharmonic equation with the clamped boundary condition by the MFS and the MAFS with $R = 5.0$, where $\epsilon = u - u_N$ or $\epsilon = u - u_N^A$.

	N	M	$\|\epsilon\|_B$	$\|\epsilon\|_{0,S}$	$\|\epsilon\|_{1,S}$	Cond	Cond_eff	$\|\mathbf{x}\|$
MFS	11	5	2.86(−2)	1.11(−2)	8.73(−2)	2.22(7)	1.69(2)	2.33(3)
	21	10	1.46(−6)	5.35(−7)	5.89(−6)	1.64(11)	6.68(5)	3.14(3)
	31	15	3.10(−11)	1.71(−11)	8.48(−11)	4.41(14)	1.79(9)	2.59(3)
NAFS with Almansi's FS	11	5	1.32(−2)	6.06(−3)	4.18(−2)	2.69(5)	6.54(2)	1.18(2)
	21	10	4.42(−7)	2.02(−7)	2.09(−6)	9.98(8)	1.79(6)	1.15(2)
	31	15	1.78(−12)	8.30(−13)	9.72(−12)	1.67(12)	2.98(9)	95.3

Table 3
Errors and condition numbers for the biharmonic equation with the clamped boundary condition by the MPS, where $\epsilon = u - u_N$.

$N = M$	$\|\epsilon\|_B$	$\|\epsilon\|_{0,S}$	$\|\epsilon\|_{1,S}$	Cond	Cond_eff	$\|\mathbf{x}\|$
5	8.24(−3)	1.73(−3)	1.44(−2)	31.6	5.74	3.25
10	4.92(−7)	1.36(−7)	1.46(−6)	3.00(2)	13.2	3.25
15	1.98(−12)	5.15(−13)	6.83(−12)	7.93(2)	7.46	3.25

Table 4
Errors and condition numbers for the biharmonic equation with the mixed type of the clamped and simply supported boundary conditions by the MFS and the MAFS with $R = 2.0$, where $\epsilon = u - u_N$ or $\epsilon = u - u_N^A$.

	N	M	$\|\epsilon\|_B$	$\|\epsilon\|_{0,S}$	$\|\epsilon\|_{1,S}$	Cond	Cond_eff	$\|\mathbf{x}\|$
MFS	11	5	1.87(−1)	2.27(−1)	1.07	1.83(4)	1.37(2)	20.3
	21	10	2.01(−3)	1.05(−3)	8.23(−3)	1.46(6)	6.48(3)	24.1
	31	15	2.62(−5)	6.33(−6)	1.08(−4)	4.87(7)	2.24(5)	19.6
	41	20	5.77(−7)	5.71(−8)	2.32(−6)	1.52(9)	7.20(6)	16.6
MAFS with Almansi's FS	11	5	4.72(−2)	3.04(−2)	1.72(−1)	1.38(3)	2.10(2)	4.35
	21	10	4.15(−4)	1.65(−4)	1.74(−3)	4.11(4)	6.58(3)	2.99
	31	15	5.00(−6)	1.04(−4)	2.02(−5)	8.35(5)	1.34(5)	2.45
	41	20	1.32(−7)	1.29(−8)	4.89(−7)	1.85(7)	2.99(6)	2.12

Table 5
Errors and condition numbers for the biharmonic equation with the mixed type of the clamped and simply supported boundary conditions by the MFS and the MAFS with $R = 5.0$, where $\epsilon = u - u_N$ or $\epsilon = u - u_N^A$.

	N	M	$\|\epsilon\|_B$	$\|\epsilon\|_{0,S}$	$\|\epsilon\|_{1,S}$	Cond	Cond_eff	$\|\mathbf{x}\|$
MFS	11	5	2.48(−2)	1.19(−2)	8.91(−2)	3.35(7)	2.59(2)	2.28(3)
	21	10	1.28(−6)	7.39(−7)	6.93(−6)	2.00(11)	8.14(5)	3.14(3)
	31	15	4.87(−11)	3.59(−11)	1.28(−10)	4.72(14)	1.92(9)	2.59(3)
MAFS with Almansi's FS	11	5	9.72(−3)	2.07(−2)	7.97(−2)	3.20(5)	8.11(2)	1.13(2)
	21	10	3.46(−7)	3.03(−7)	2.46(−6)	1.04(9)	1.86(6)	1.15(2)
	31	15	1.45(−12)	1.04(−12)	1.20(−11)	1.79(12)	3.19(9)	95.3

Table 6
Errors and condition numbers for the biharmonic equation with the mixed type of the clamped and simply supported boundary conditions by the MPS, where $\epsilon = u - u_N$.

$n = M$	$\|\epsilon\|_B$	$\|u - u_n\|_{0,S}$	$\|u - u_n\|_{1,S}$	Cond	Cond_eff	$\|\mathbf{x}\|$
5	1.04(−2)	3.34(−3)	2.05(−2)	29.4	4.99	3.25
10	5.50(−7)	1.51(−7)	7.11(−12)	8.70(2)	7.93	3.25
15	2.32(−12)	6.06(−13)	7.11(−12)	8.70(2)	7.93	3.25

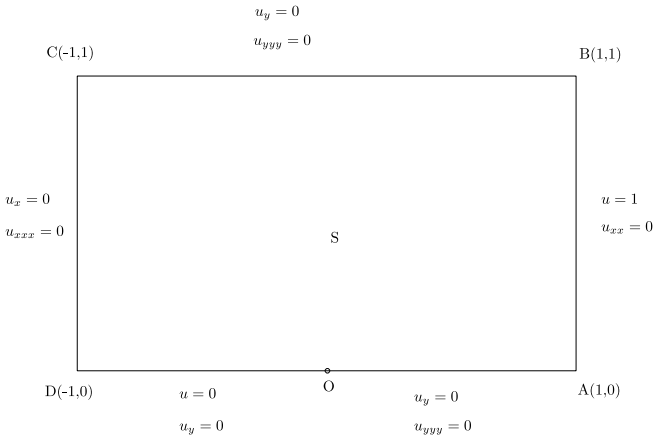

Fig. 1. Model II called in [6].

required, where ν is the outward normal direction to the boundary ∂S. On $\overline{AB}$ when the simply supported conditions are provided, we choose the biharmonic equation with the following boundary condition, called Model II in [6] and also in this paper, see Fig. 1

$$\begin{aligned} &u|_{\overline{OD}} = 0, \quad u_y|_{\overline{OD}} = 0, \quad u_y|_{\overline{OA}} = 0, \quad u_{yyy}|_{\overline{OA}} = 0, \\ &u|_{\overline{AB}} = 1, \quad u_{xx}|_{\overline{AB}} = 0, \quad u_y|_{\overline{BC}} = 0, \quad u_{yyy}|_{\overline{BC}} = 0, \quad u_x|_{\overline{CD}} = 0, \quad u_{xxx}|_{\overline{CD}} = 0. \end{aligned} \tag{5.1}$$

There exists a singularity at O due to the intersection of the clamped and simply supported boundary conditions. The true function can be found as in [6,12]

$$u = \sum_{i=1}^{\infty} (d_i g_i(r,\theta) + c_i f_i(r,\theta)), \tag{5.2}$$

where

$$g_i(r,\theta) = r^{i+1/2} \left\{ \cos\left(i - \frac{3}{2}\right)\theta - \frac{i - \frac{3}{2}}{i + \frac{1}{2}} \cos\left(i + \frac{1}{2}\right)\theta \right\}, \tag{5.3}$$

$$f_i(r,\theta) = r^{i+1}\{\cos(i-1)\theta - \cos(i+1)\theta\}. \tag{5.4}$$

To compute the errors of MFS, we choose the highly accurate solution $u_{30} = \sum_{i=1}^{30}(d_i g_i(r,\theta) + c_i f_i(r,\theta))$ as the exact solution u, where the coefficients d_i and c_i are also given in [6]. For the boundary condition (5.1), define an energy on the boundary by

$$\begin{aligned} I(v) = &\int_{\overline{AB}} ((v-1)^2 + w_2^2 v_{xx}^2) + \int_{\overline{BC}} (w_1^2 v_y^2 + w_3^2 v_{yyy}^2) \\ &+ \int_{\overline{CD}} (w_1^2 v_x^2 + w_3^2 v_{xxx}^2) + \int_{\overline{OA}} (w_1^2 v_y^2 + w_3^2 v_{yyy}^2) + \int_{\overline{DO}} (v^2 + w_1^2 v_y^2), \end{aligned} \tag{5.5}$$

where the weight $w_i = O\left(\frac{1}{N^i}\right)$, and $2N$ is the number of fundamental solution terms. We use midpoint method to approximate (5.5). In computation, we use only the MFS with (1.8), and choose $R = 1.6$ and $R = 2.0$. In this subsection, the source points are uniformly located on the outside circle $l_R = \{(r,\theta) | r = R, 0 \le \theta \le 2\pi\}$, where $R > r_{\max}$ and $r_{\max} = \frac{\sqrt{5}}{2}$. Since the FS in (1.6) and (1.7) are smooth on ∂S, the local refinements of collocation nodes P_i near O should be used (see [13]). The errors and condition numbers are listed in Tables 7 and 8. From Fig. 2, it is shown that the derivatives of these numerical solutions are large and undesirable. Then we may improve the MFS by greedy adaptive techniques in the next subsection, to select the source points differently.

5.2. Greedy adaptive techniques to select source points

Greedy adaptive techniques are the algorithms to select better source points, which were first introduced for radial basis functions in [14], and then for the MFS in [15,16]. The idea is as follows. First we assume many potential source points, as shown in Fig. 3. Then we select the effective source points, based on smaller errors. For the potential source points as shown in Fig. 3, we obtain $\mathbf{Fx} = \mathbf{b}$, where $\mathbf{F} = R^{m\times n}$. Then we reduce n as small as possible, to pick up the useful columns of the

Table 7
Errors and condition numbers for Model II with $R = 1.6$ and $M = 55$ by the MFS, where $\varepsilon = u - u_N$, $2N$ is the number of FS terms, and M is the number of collocation points of $\overline{AB}$.

N	10	20	30	40	50
$\|\varepsilon\|_B$	1.84(−1)	3.59(−2)	1.17(−2)	1.17(−2)	7.31(−3)
$\|\varepsilon\|_{\infty,\overline{AB}\cup\overline{DO}}$	1.79(−1)	7.99(−2)	5.37(−2)	3.49(−2)	2.50(−2)
$\|\varepsilon_\nu\|_{\infty,\overline{AD}\cup\overline{BC}\cup\overline{CD}}$	1.50(−1)	9.78(−2)	6.42(−2)	4.90(−2)	4.41(−2)
$\|\varepsilon_{\nu\nu}\|_{\infty,\overline{AB}}$	2.00(−1)	3.38(−2)	6.41(−2)	2.58(−2)	6.45(−2)
$\|\varepsilon_{\nu\nu\nu}\|_{\infty,\overline{OA}\cup\overline{BC}\cup\overline{CD}}$	7.15(−1)	9.67(−1)	1.51	4.04	4.68
$\|\varepsilon\|_{0,S}$	1.23(−1)	5.29(−2)	4.46(−2)	6.48(−2)	7.06(−2)
$\|\varepsilon\|_{1,S}$	4.35(−1)	2.20(−1)	1.77(−1)	1.90(−1)	1.88(−1)
Cond	2.23(2)	1.03(5)	1.51(7)	1.64(9)	1.21(11)
Cond_eff	19.53	1.39(2)	1.85(2)	1.22(3)	3.66(3)
$\|\mathbf{x}\|_2$	68.7(−1)	4.01(1)	4.37(3)	5.35(4)	1.19(6)

Table 8
Errors and condition numbers for Model II with $R = 2.0$ and $M = 55$ by the MFS, where $\varepsilon = u - u_N$, $2N$ is the number of FS terms, and M is the number of collocation points of $\overline{AB}$.

N	10	20	30	40
$\|\varepsilon\|_B$	1.12(−1)	3.56(−2)	2.10(−2)	1.18(−2)
$\|\varepsilon\|_{\infty,\overline{AB}\cup\overline{DO}}$	1.84(−1)	8.31(−2)	5.38(−2)	3.50(−2)
$\|\varepsilon_\nu\|_{\infty,\overline{AD}\cup\overline{BC}\cup\overline{CD}}$	1.00(−2)	9.52(−2)	8.24(−2)	5.59(−2)
$\|\varepsilon_{\nu\nu}\|_{\infty,\overline{AB}}$	1.41(−1)	1.37(−1)	9.57(−2)	5.78(−2)
$\|\varepsilon_{\nu\nu\nu}\|_{\infty,\overline{OA}\cup\overline{BC}\cup\overline{CD}}$	1.50(−1)	8.86(−2)	1.78	3.82
$\|\varepsilon\|_{0,S}$	1.31(−1)	6.85(−2)	3.83(−2)	6.39(−2)
$\|\varepsilon\|_{1,S}$	4.48(−1)	2.45(−1)	1.67(−1)	1.87(−1)
Cond	1.05(3)	6.53(3)	2.11(8)	3.61(10)
Cond_eff	2.13(1)	5.73(1)	2.87(2)	7.30(2)
$\|\mathbf{x}\|_2$	2.04	1.63(2)	1.47(4)	1.61(6)

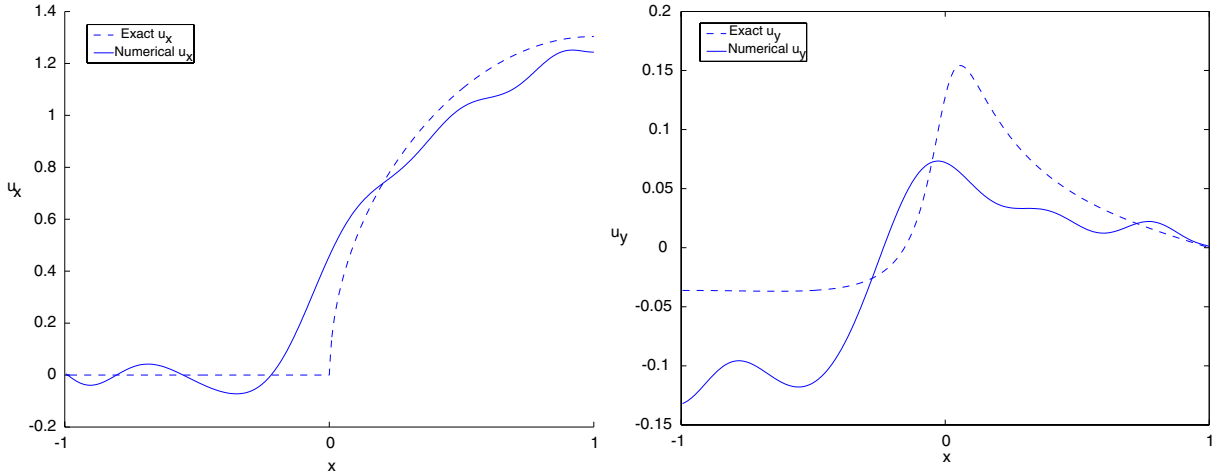

Fig. 2. Numerical derivatives $u_x|_{y=0}$ and $u_y|_{y=0}$ by the MFS ($N = 80$ and $R = 1.6$) without greedy adaptive techniques, where the source points are uniformly located on the outside circle l_R.

$m \times n$ matrix $\mathbf{F}$ in a data-dependent way without cutting the number m of rows down for $\mathbf{Fx} = \mathbf{b}$. To maintain stability, we use orthogonal transformations, but choose the columns dependent on the right-hand side vector $\mathbf{b}$.

Let $\mathbf{F} = (\mathbf{f}_1, \ldots, \mathbf{f}_n)$, where $\mathbf{f}_i$ are the column vectors. To approximate $\mathbf{b}$ by multiples of a nonzero vector $\mathbf{f}$, the error vector is given by $\mathbf{b} - \mathbf{f} \cdot \frac{\mathbf{b}^T\mathbf{f}}{\mathbf{f}^T\mathbf{f}}$. We may find j such that the error

$$\|\mathbf{b}\|_2 - \frac{(\mathbf{b}^T\mathbf{f}_j)^2}{\|\mathbf{f}_j\|_2^2}, \quad 1 \le j \le n,$$

is minimal, where $\|\mathbf{b}\|_2$ is the Euclidean norm. This is equivalent to choose the maximum of the values:

$$\frac{(\mathbf{b}^T\mathbf{f}_j)^2}{\|\mathbf{f}_j\|^2}, \qquad \|\mathbf{f}_j\|_2^2 \neq 0.$$

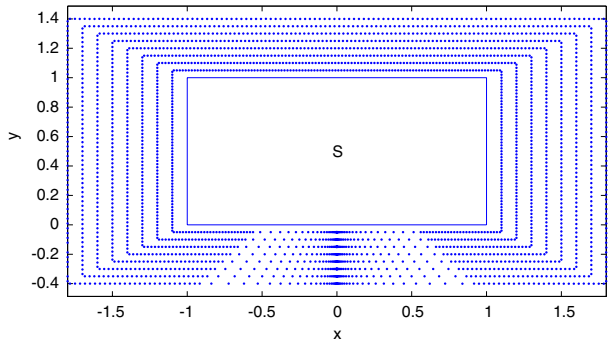

Fig. 3. The initial source points.

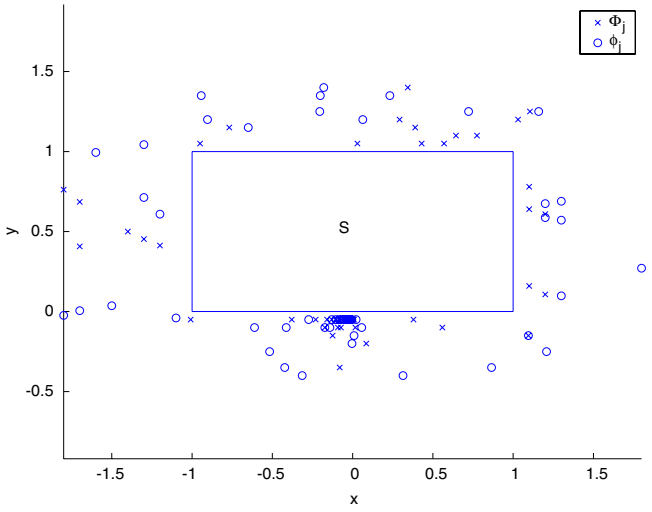

Fig. 4. The $100(=N_1+N_2)$ source points selected by Algorithm I.

So we have Algorithm I given in Appendix (also see [14–16]), and apply it to our problem. Note that the local refinements of collocation nodes near the singular point O can also be applied. Since the final source points are different for the Φ_j and ϕ_j after the greedy adaptive techniques, the FS solutions in (1.8) are modified as

$$v_N = \sum_{j=1}^{N_1} c_j \Phi_j(r,\theta) + \sum_{j=1}^{N_2} d_j \phi_j(r,\theta). \tag{5.6}$$

The initial and final source points are drawn in Figs. 3 and 4, respectively. From Fig. 4, we can see that there exist more source points selected near to the singular point O; such results coincide with [15,16]. The numerical results are listed in Table 9 with $N = \frac{1}{2}(N_1+N_2)$, and the error curves are drawn with Figs. 5 and 6. From Table 9, we can see the following asymptotic relations,

$$|\varepsilon|_B \approx O(0.90^N), \qquad \|\varepsilon\|_{0,S} \approx O(0.96^N), \qquad \|\varepsilon\|_{1,S} \approx O(0.96^N),$$
$$\text{Cond} \approx O(1.58^N), \qquad \text{Cond\_eff} \approx O(1.08^N),$$

where $\varepsilon = u - u_N$, and the effective condition number is given in (4.4).

From Tables 8 and 9 at $N = 40$, we cite the errors:

$$\|\varepsilon\|_{0,S} = 6.39(-2), \qquad \|\varepsilon\|_{1,S} = 1.87(-1), \quad \text{in Table 8},$$
$$\|\varepsilon\|_{0,S} = 1.01(-2), \qquad \|\varepsilon\|_{1,S} = 3.62(-2), \quad \text{in Table 9},$$

and the condition numbers:

$$\text{Cond} = 3.61(10), \qquad \text{Cond\_eff} = 7.30(2), \quad \text{in Table 8},$$
$$\text{Cond} = 1.52(8), \qquad \text{Cond\_eff} = 2.90(3), \quad \text{in Table 9}.$$

Hence, the errors of solutions and derivatives by the MFS using the greedy adaptive techniques are smaller, while the condition numbers are smaller but the effective condition numbers are larger. Comparing Figs. 5 and 6 with Fig. 2 in

Table 9
Errors and condition numbers for Model II by the MFS with greedy adaptive techniques, where $\varepsilon = u - u_N$, $N = \frac{1}{2}(N_1 + N_2)$, $2N$ is the number of FS terms, and $M = 55$ is number of collocation points on $\overline{AB}$.

N	10	20	30	40	50	60
$\|\varepsilon\|_B$	6.20(−2)	8.23(−3)	1.61(−3)	6.49(−4)	2.21(−4)	1.19(−4)
$\|\varepsilon\|_{0,S}$	1.31(−1)	3.56(−2)	1.60(−2)	1.01(−2)	6.37(−3)	4.56(−3)
$\|\varepsilon\|_{1,S}$	4.33(−1)	1.30(−1)	5.47(−2)	3.62(−2)	2.36(−2)	1.68(−2)
Cond	6.84(3)	1.08(4)	6.46(6)	1.52(8)	1.56(10)	4.45(13)
Cond_eff	19.3	2.39(2)	1.21(3)	2.90(3)	5.53(3)	2.10(4)
$\|\mathbf{x}\|_2$	1.86	2.32	1.98(2)	2.35(3)	1.66(5)	1.30(8)

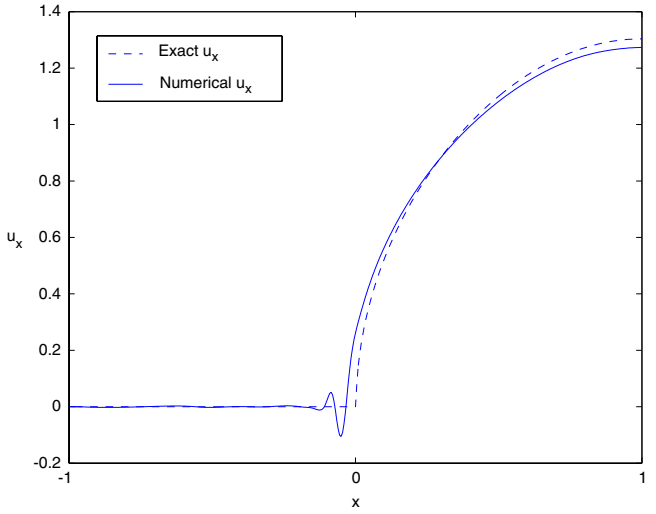

Fig. 5. Numerical derivatives $u_x|_{y=0}$ and $u_y|_{y=0,1}$ by the MFS ($N_1 + N_2 = 80$) with greedy adaptive techniques.

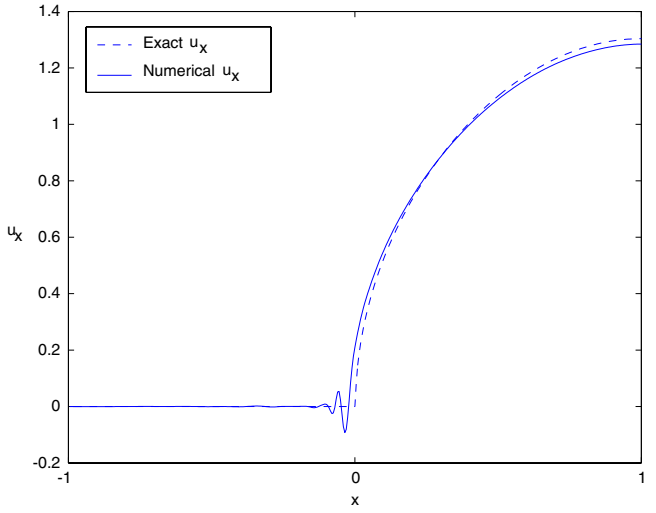

Fig. 6. Numerical derivatives $u_x|_{y=0}$ and $u_y|_{y=0,1}$ by the MFS ($N_1 + N_2 = 100$) with greedy adaptive techniques.

Section 5.1, the derivative curves are significantly closer to the true curves. Although the greedy adaptive techniques need more CPU time, the source points selected by the greedy adaptive techniques are advantageous for the MFS for the biharmonic equation with singularity.

Finally in Table 10, we cite the results of the MPS from [12]. From Table 10, we can see that

$$|\varepsilon|_B = O(0.59^N), \qquad \text{Cond} = O(1.55^N), \qquad \text{Cond\_eff} = O(1.09^N).$$

Table 10
The computed results by the MPS from [12], where $\varepsilon = u - u_N$, $2N$ is the number of PS terms, and $\sigma_{\max}$ and $\sigma_{\min}$ are the maximal and minimal singular values of the discrete matrix **F**, respectively.

N	M	$\lvert\varepsilon\rvert_B$	Cond	Cond_eff	$\sigma_{\max}$	$\sigma_{\min}$
5	40	3.33(−3)	228	41.7	6.29	2.76(−2)
10	80	5.68(−5)	6.78(3)	268	29.2	4.32(−3)
15	120	2.80(−6)	1.06(5)	820	150	1.41(−3)
20	160	1.38(−7)	1.11(6)	1.86(3)	692	6.23(−4)
25	200	3.30(−9)	9.61(6)	3.55(3)	3.14(3)	3.27(−4)
30	240	2.34(−10)	9.58(7)	6.04(3)	1.84(4)	1.92(−4)
35	280	1.51(−11)	8.60(8)	9.46(3)	1.05(5)	1.23(−4)

Comparing Table 10 with Tables 7–9, the solutions of the MPS are significantly more accurate than those of the MFS even using the greedy adaptive techniques. Such conclusions can be seen from the data cited from Tables 9 and 10:

$$|\varepsilon|_B = 6.49(-4), \quad \text{Cond} = 1.52(8), \quad \text{Cond\_eff} = 2.90(3), \quad \text{in Table 9 at } N = 40,$$
$$|\varepsilon|_B = 1.15(-11), \quad \text{Cond} = 8.60(8), \quad \text{Cond\_eff} = 9.46(3), \quad \text{in Table 10 at } N = 35.$$

Remark 5.1. Better choice of source points is an important issue for the MFS. In [17–19], for Laplace's equation on the disk domain $S_\rho = \{(r,\theta) | r \le \rho, 0 \le \theta \le 2\pi\}$, the source points Q_j^* are uniformly located on the larger circle $l_R (R > \rho)$, and the exponential convergence rates of the MFS are derived for smooth solutions. In [20], a better choice of source points is explored for the bounded simply connected domain S as follows. By a conformal mapping T, the S can be transformed to a disk domain S_ρ, and the source points Q_j are obtained by the inverse conforming mapping: $Q_j = T^{-1}Q_j^*$. Such techniques have been implemented numerically for the MFS for the singularity problems: the biharmonic equation with the boundary conditions (5.1). The computed results do not show a better behavior than the MFS using the uniform source points directly on l_R; details are omitted. Hence, the techniques in [20] for choosing source points may not be helpful for the MFS for singularity problems. Based on the computed results in this subsection, the greedy adaptive techniques are recommended.

Remark 5.2. To conclude this section, let us discuss the relations among MFS, MAFS and MPS. We classify them as the Trefftz method described in (1.9) but with different admissible functions in V_N, such as FS, with Almansi's FS and PS. Numerical experiments and comparisons are reported in [21] for smooth solutions, to show that the MFS and MAFS achieve the equivalent convergence rates by the MPS, but offer much larger condition numbers. Such comparisons retain the same for singularity problems shown in this paper. These results coincide with the analysis in Sections 2 and 3, where the optimal convergence rates and the exponential growth rates of Cond are derived. In [22,23], a similarity (but not an intrinsic equivalence) of algorithms between MFS and MPS is discovered for Laplace and biharmonic equations. The fundamental solutions can be expanded into particular solutions (such as harmonic or biharmonic polynomials; see [24]), and a particular solution can also be expressed as a linear combination of FS; see Section 2. However, the bounds of their errors and condition numbers are distinct; see the analysis in Sections 2 and 3. In [25,26], the series expansions of FS are fully used for the null field method (NFM) for circular domains with circular holes, where the semi-analytic solutions are obtained. Their explicit discrete algorithms and strict analysis will be reported in another paper.

6. Concluding remarks

To conclude this paper, let us make a few concluding remarks.

1. In this paper, the method of fundamental solution (MFS) is used for biharmonic equations with both smooth and singular solutions. Both the traditional FS as $r_j^2 \ln r_j$ and Almansi's FS as $\rho^2 \ln r_j$ are chosen for the MFS, the latter is denoted as the MAFS.
2. The error analysis for the MAFS is made in Section 2, to give the polynomial convergence rates, and in Section 3, the stability analysis of the MAFS is also made for circular domains, to give the exponential growth rates of condition number. Their numerical results in Section 4 are slightly better than those by the MFS. Hence, we may simply choose the MAFS with (1.12) for engineering applications. It is noteworthy to pointing out that this paper is the first time to explore the analysis of the MAFS and to compare the MAFS with the traditional MFS.
3. For the biharmonic equation with smooth solutions, the clamped and the mixed boundary conditions are considered. The MFS, the MAFS and the MPS (i.e., the Trefftz method using the particular solutions) are used, and the source points are uniformly located on the enlarged circle l_R with $R > r_{\max}$. The errors of the MFS and the MAFS can cope with those of the MPS, if the instability will not adversely affect the accuracy. However, in computation with double precision in Section 4, the MPS is superior to both MFS and MAFS, due to better stability.
4. For the biharmonic equations with crack singularity, the MPS results are given in [6]. We use the MFS with source points on circles with local refinements of collocation nodes, and the computed results are not satisfactory; see Fig. 2. In general, adding one or two particular solutions is useful. Whenever we find the particular solutions of the problem, we should choose the MPS. However, for singularity problems, if the singular particular solutions cannot be found, we may adapt

the MFS by the local refined collocation nodes, and by selecting the source points from the greedy adaptive techniques. From the numerical results in Section 5.2, the greedy adaptive techniques may provide better solutions for singularity problems.

Acknowledgments

We express our thanks to J.T. Chen for valuable comments and suggestions. We are also indebted to T.C. Wu for the computation in this paper.

Appendix

Algorithm I.

*Step*1: Pick the column of **F** whose multiples approximate **b** best:

1. *Copy* $\mathbf{F} \to \mathbf{A}$.
2. *Find j such that* $\frac{(\mathbf{b}^T\mathbf{a}_j)^2}{\|\mathbf{a}_j\|_2^2}$ *is maximal and* $\|\mathbf{a}_j\|_2 \neq 0$.
3. *Set* $\mathbf{u} = \mathbf{a}_j$, and $\mathbf{v} = \mathbf{u}/\|\mathbf{u}\|_2$.
4. *Store j*.

*Step*2: Transform the problem to the space orthogonal to the column:

5. $\mathbf{A} = \mathbf{A} - \mathbf{v}(\mathbf{v}^T)\mathbf{A}$.
6. $\mathbf{b} = \mathbf{b} - \mathbf{v}(\mathbf{v}^T)\mathbf{b}$.

If the satisfactory solution is obtained, the computation is terminated; otherwise repeat *Steps* 1 *and* 2.

References

[1] Z.C. Li, T.T. Lu, H.Y. Hu, A.H.-D. Cheng, Trefftz and Collocation Methods, WIT, Southsampton, Boston, 2008.
[2] G. Fairweather, A. Karageorghis, The method of fundamental solutions for elliptic boundary value problems, Adv. Comput. Math. 9 (1998) 69–95.
[3] A. Karageorghis, G. Fairweather, The Almansi method of fundamental solutions for solving biharmonic problems, Internat. J. Numer. Methods Engrg. 26 (1988) 1665–1682.
[4] A. Karageorghis, G. Fairweather, The simple layer potential method of fundamental solutions for certain biharmonic problems, Int. J. Numer. Methods Fluids 9 (1989) 1221–1234.
[5] A. Karageorghis, G. Fairweather, The method of fundamental solutions for the numerical solution of biharmonic equation, J. Comput. Phys. 69 (1998) 434–459.
[6] Z.C. Li, T.T. Lu, H.Y. Hu, The collocation Trefftz method for biharmonic equations with singularities, Eng. Anal. Bound. Elem. 28 (2004) 79–96.
[7] A. Bogomolny, Fundamental solutions method for elliptic boundary value problems, SIAM J. Numer. Anal. 22 (1985) 644–669.
[8] Z.C. Li, Method of fundamental solutions for annular shaped domains, J. Comput. Appl. Math. 228 (2009) 355–372.
[9] Z.C. Li, H.T. Huang, J. Huang, Stability analysis of method of fundamental solutions for mixed boundary value problems of Laplace's equations, Computing 88 (2010) 1–29.
[10] P. Davis, Circulant Matrices, John Wiley & Sons, New York, 1979.
[11] Z.C. Li, C.S. Chien, H.T. Huang, Effective condition number for finite difference method, J. Comput. Appl. Math. 198 (2007) 208–235.
[12] Z.C. Li, T.T. Lu, Y. Wei, Effective condition number of Trefftz methods for biharmonic equations with crack singularities, Numer. Linear Algebra 16 (2009) 145–171.
[13] Z.C. Li, The fundamental solutions for Laplace's equation with mixed boundary condition, in: C.S. Chen, A. Karageorghis, Y.S. Smyrlis (Eds.), The Method of Fundamental Solutions—A Meshless Method, Dynamic Publishers, Inc., USA, 2009, pp. 29–49. Chapter 2.
[14] R. Schaback, H. Wenland, Adaptive greedy techniques for approximate solution on large RBF systems, Numer. Algorithms 24 (2000) 239–254.
[15] L. Ling, R. Opfer, R. Schaback, Results on meshless collocation techniques, Eng. Anal. Bound. Elem. 30 (2006) 247–253.
[16] R. Schaback, Adaptive numerical solution of MFS systems, a plenary talk at the first Inter. Workshop on the Method of Fundamental Solutions (MFS2007), Ayia Napa, Cyprus, June 11–13, 2007, in: C.S. Chen, A. Karageorghis, Y.S. Smyrlis (Eds.), The Method of Fundamental Solutions—A Meshless Method, Dynamic Publishers, Inc., USA, 2009, pp. 1–28. also as Chapter 1.
[17] M. Katsurada, A mathematical study of the charge simulation method II, J. Fac. Sci. Univ. Tokyo, Sect. IA. Math. 36 (1989) 135–162.
[18] M. Katsurada, Asymptotic error analysis of the charge simulation method in a Jordan region with an analytical boundary, J. Fac. Sci. Univ. Tokyo, Sect. IA. Math. 37 (1990) 635–657.
[19] M. Katsurada, Charge simulation method using exterior mapping functions, Japan J. Indust. Appl. Math. 11 (1994) 47–61.
[20] M. Katsurada, H. Okamoto, The collocation points of the method of fundamental solutions for the potential problem, Comput. Math. Appl. 31 (1996) 123–137.
[21] Z.C. Li, H.J. Young, H.T. Huang, Y.P. Liu, A.H.-D. Cheng, Comparisons of fundamental solutions and particular solutions for Trefftz methods, Eng. Anal. Bound. Elem. 34 (2010) 248–258.
[22] J.T. Chen, C.S. Wu, Y.T. Lee, K.H. Chen, On equivalence of Trefftz method of fundamental solutions for Laplace and biharmonic equations, Comput. Math. Appl. 53 (2007) 851–879.
[23] J.T. Chen, Y.T. Lee, S.R. Yu, S.C. Shieh, Equivalence between Trefftz method and method of fundamental solution for annular Green's function using the addition theorem and image concept, Eng. Anal. Bound. Elem. 33 (2009) 678–688.
[24] Z.C. Li, M.G. Lee, J.T. Chen, New series expansions of fundamental solutions of linear elastostatics, Computing (2010) (in press).
[25] J.T. Chen, S.R. Kuo, J.H. Lin, Analytic study and numerical experiments for degenerate scale problems in the boundary element method for two-dimensional elasticity, Internat. J. Numer. Methods Engrg. 54 (2002) 1669–1681.
[26] J.T. Chen, C.C. Hsiao, S.Y. Leu, Null-field integral equation approach for plate problems with circular boundaries, J. Appl. Mech. 73 (2006) 679–693.